

THE PREPARATION OF CARBON NANOFIBERS SUPPORTED NICKEL NANOPARTICLES AND THEIR CATALYTICAL PROPERTIES

G. WAN, X. PENG, G. WANG*

Key Laboratory of Advanced Materials of Tropical Island Resources (Hainan University), Ministry of Education, Haikou 570228, P. R. China

Carbon nanofibers supported nickel (Ni/CNFs) were prepared by means of a microwave-assisted process, in which the Ni salts are reduced by hydrazine hydrate in a water/ethylene glycol system and deposited onto carbon nanofibers (CNFs). The phase structures and morphologies of the composites have been characterized by X-ray diffraction, field-emission scanning electron microscopy and high-resolution transmission electron microscopy. The results show that a dense and homogeneous layer of nickel nanoparticles with an average diameter about 18.4 nm on CNFs can be obtained. Magnetization curves demonstrate that the as-prepared Ni/CNFs are ferromagnetic and that the coercivity is 102 Oe. In addition, initial concentration of hydrazine hydrate has an important effect on the nickel nanoparticle size of the resulting product. The catalytic behavior in selective hydrogenation of *p*-nitrophenol (PNP) to *p*-aminophenol (PAP) was studied. It was found that the catalytic activities of the Ni/CNFs were increased with lessening of average particles size of nickel nanoparticle on the surface of CNFs, but little influence on the selectivity. As compared to the conventional RANEYs Ni catalyst, all the Ni/CNFs showed higher catalytic activity and selectivity in the hydrogenation of PNP to PAP.

(Received April 29, 2017; Accepted July 7, 2017)

Keywords: Ni/CNFs; Magnetic properties; Catalytic activity; PNP hydrogenation

1. Introduction

p-Aminophenol (PAP) is of great commercial importance as an intermediate for the preparation of several analgesic and antipyretic drugs such as paracetamol, acetanilide, phenacetin, and so forth [1-4]. The traditional synthesis routes are usually harmful to the environment. Direct hydrogenation of *p*-nitrophenol (PNP) catalyzed by metal nanoparticles is considered as an alternative green process for the preparation of PAP [5,6]. Among of them, nickel-based catalysts have been of great interest, because of exhibited excellent catalytic activity in the selective hydrogenation reaction of PNP to PAP. Up to now, some works have been reported on the PNP hydrogenation over nickel-based catalysts [5,7-13]. For instance, Li et al. [7] prepared nickel nanoparticles supported on boehmite by a modified electroless nickel-plating method and a direct reduction method. The as-prepared catalysts exhibited superior activity attributed to the small Ni-B particles and greater content of structural water, which enhanced the hydrophilicity of the catalyst. Yin and coworkers [8-10] reported the synthesis of phase pure nickel nanoparticles with facile size and structure controlled using different organic modifiers and all of the nickel nanoparticles showed higher catalytic activity and selectivity than the conventional RANEYs Ni catalyst in the hydrogenation of PNP to PAP. In addition, SiO₂-Al₂O₃ supported nano-sized nickel was prepared by sol-gel method and the results showed that the degree of crystallinity of the support affects the catalytic activity of nano-sized Ni catalyst [11].

*Corresponding author: wangguizhen0@hotmail.com

Recently, carbon nanofibers (CNFs) supported metal catalysts have received significant research attention due to the range of applications. A variety of metal catalysts have been prepared on CNFs support and tested in important industrial reactions. Of particular interest are carbon nanofibers supported nickel (Ni/CNFs) [14-19] with good dispersion and controlled size, because of their relatively high catalytic activity and selectivity to a lot of reactions. However, the catalytic performance of Ni/CNFs in the hydrogenation of PNP to PAP was seldom investigated until now.

Herein, we report a simple microwave-assisted procedure for the assembly of a compact layer of magnetic nickel nanoparticles onto CNFs in a water/ethylene glycol (EG) system. The as-prepared Ni/CNFs catalysts show higher catalytic activity and selectivity in the hydrogenation of PNP to PAP compared with that of conventional Raney Ni catalyst. Moreover, it was found that support particle size has significant influences on catalytic activity of the resulting catalyst.

2. Experimental

The CNFs used in this study were synthesized by a low temperature (300 °C) nano-copper catalytic chemical vapor deposition method [20,21]. All of the chemicals used in the experiments are analytical grade without further purification.

2.1 Preparation of composites

The starting CNFs were subjected to an oxidation treatment in the nitric acid to modify the surface chemistry and dispersive property. A two-step pretreatment, sensitization and activation, was used to catalyze the CNFs. The sensitizer and activator were stannous chloride/hydrochloric acid (15 g L⁻¹ SnCl₂·2H₂O and 41 g L⁻¹ HCl) and palladium chloride/hydrochloric acid (0.5 g L⁻¹ PdCl₂ and 12 g L⁻¹ HCl) solutions, respectively. Ultrasonic vibration was applied during the catalyzation treatment to facilitate uniform activation throughout the entire surface of CNFs.

In a typical experiment to prepare Ni/CNFs catalysts, 0.5 g of CNFs and 0.15 g of NiCl₂·6H₂O were dispersed in 40 mL of EG by ultrasonic vibration for 0.5 h. 0.24 g of N₂H₄·H₂O (80 wt. %) solution was added dropwise to the solution, followed by the addition of 2 ml of 0.25 M L⁻¹ NaOH aqueous solution. 60% (450 W) of the output power of the microwave was used to irradiate the mixture for 5 min. Then, the microwave heating was terminated and the products were collected by centrifugation, washed with distilled water and absolute ethanol repeatedly for three times, and dried at 45 °C in vacuum.

2.2. Catalyst Characterization

X-ray powder diffraction (XRD) analysis was performed on a BRUKER AXS D8 Advance diffractometer with Cu K α radiation ($\lambda = 1.54178 \text{ \AA}$) using a 40 kV operation voltage and 40 mA current. Scanning electron microscopy (SEM) was recorded on a JEOL JSM-6700F field-emission scanning electron microscope (FE-SEM). The transmission electron microscopy (TEM) and high-resolution transmission electron microscopy (HRTEM) images were collected on a JEOL JEM 2100 transmission electron microscope operating at an accelerating voltage of 200 kV. Magnetic properties were recorded in a Quantum Design vibrating sample magnetometer (VSM) at room temperature.

2.3. Catalyst Testing

The hydrogenation of PNP was carried out in a 100 mL autoclave fitted with a magnetically driven impeller. The autoclave contained 0.1 g the as-prepared Ni/CNFs or Raney Ni catalyst, 3 g *p*-nitrophenol, 20 mL ethanol, and 10 mL distilled water were mixed. After replacing the air in the reactor with H₂, the reaction was performed at 373 K and hydrogen pressure of 0.8 MPa with stirring at 800 rpm. The liquid phase sample was analyzed by high-performance liquid chromatography (HPLC, Waters 2695).

3. Results and discussion

The XRD pattern of as-synthesized Ni/CNFs is shown in Fig. 1. A broad diffraction line at 20-40° reveals the graphite-like character of the CNFs. The diffraction peaks at $2\theta = 44^\circ$, 51° and 76° can be assigned to (111), (200) and (220) planes of nickel (JCPDS 88-0866), respectively. The diameter of nanoparticles characterized from Scherrer formula is 18.1 nm. No other diffraction peaks can be found, indicating that the coating layer on the surface of CNFs is only composed of nickel nanoparticles.

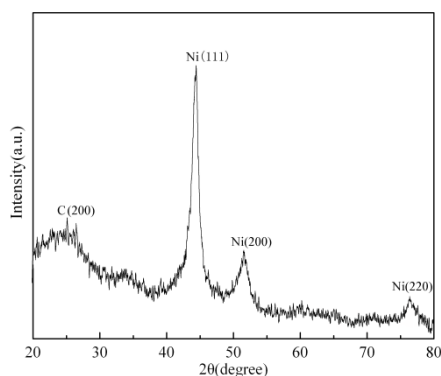


Fig. 1. XRD pattern of as-synthesized Ni/CNFs.

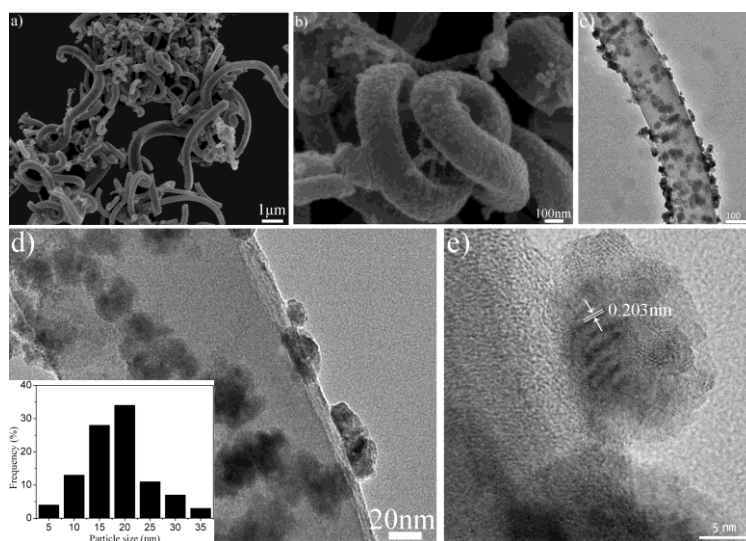


Fig. 2. (a, b) SEM, (c, d) TEM and (e) HRTEM images of the as-synthesized Ni/CNFs. The inset shows the histogram of the nickel nanoparticles size distribution (more than 100 nanoparticles were measured).

Fig. 2 displays SEM and TEM images of Ni/CNFs. As the SEM images shown in Fig. 2(a, b), the CNFs are 50-200 nm in diameter and homogeneously coated by the dense layer of nickel nanoparticles. Fig. 2(c, d) shows an individual CNF which was coated by nickel nanoparticles. Clearly, the sample contains well-dispersed nickel particles with a narrow size distribution on the surface of the CNF. The histogram in the inset to Fig. 2d shows a size distribution between 5 and 35 nm with an average diameter about 18.4 nm, which are in close agreement with the result of XRD diffraction pattern. The HRTEM image (Fig. 2e) further reveals a group of 2D lattice fringes, and interplanar spacing is measured to be 0.203 nm, corresponding to the (111) plane of nickel.

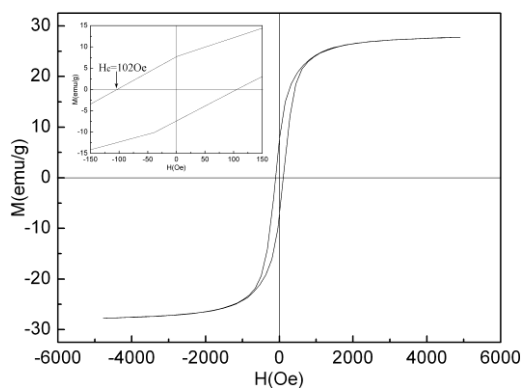


Fig. 3. Hysteretic loop at room temperature of the as-synthesized Ni/CNFs.

e determined using a vibrating sample magnetometer. It is clear to be seen from Fig. 3 that the as-synthesized Ni/CNFs is ferromagnetic. The saturation magnetization (M_s) of magnetic composites is 27.8 emu/g, considerably smaller than that of bulk nickel ($M_s = 55$ emu/g) [22]. The curve of the as-synthesized products, as assumed, mainly displays the magnetic contribution of nickel nanoparticles deposited on the CNFs. Thus, the Ni/CNFs is ferromagnetic with sizes beyond the super paramagnetic limit, which is 15 nm for spherical nickel nanoparticles [23]. As can be seen from inset to Fig. 3, the Ni/CNFs exhibited remarkable enhancement in coercivity (102 Oe) compared with that of bulk nickel (ca. 0.7 Oe) [22,24]. It is known that the coercivity of magnetic materials depends strongly on various types of anisotropy (crystal anisotropy, shape anisotropy, stress anisotropy, externally induced anisotropy, and exchange anisotropy), among which the shape anisotropy is predicted to produce the largest coercive forces [25]. Therefore, the higher coercivity in the present work can be attributed to the shape and stress anisotropy of nickel chains supported by the long CNFs.

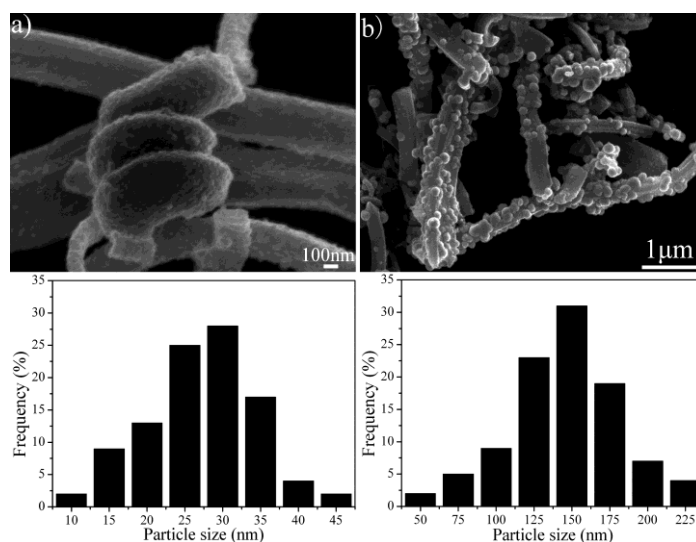
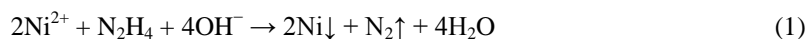


Fig. 4. SEM images of Ni/CNFs in the presence of 0.36 g (a) and 0.12 g (b) of hydrazine hydrate. The histograms under the SEM images show corresponding size distribution of the nickel nanoparticles.

It is well known that nickel can be formed through the reaction between Ni^{2+} and N_2H_4 in aqueous solution. The reaction process is expressed as the following equation:



When all reactants were introduced into a solution, the nickel nanoparticles would form on the surface of CNFs by the above process. To find the effect of the amount of hydrazine hydrate on the products, the experiment was carried out in the addition of various amounts of hydrazine hydrates, while keeping other experimental conditions unchanged. When 0.36 g of hydrazine hydrate was used, as shown in Fig. 4a, the surface of CNFs is sparsely decorated with nickel nanoparticles, and the average diameter of nickel nanoparticles determined from the corresponding histogram is 27.3 nm. Fig. 4b shows the product obtained with 0.12 g hydrazine hydrate. The average diameter of nickel nanoparticles revealed from the corresponding histogram is about 145 nm. It indicates that the particle size is sensitive with the amount of the hydrazine hydrate.

These results can be explained by the reaction rate on the nucleation. It is known that the average particle size decreases with increasing the nuclei concentration in the solution due to suppressing the growth of particles by the formation of many nuclei in the period of nucleation step. Additionally, when most nuclei are formed at the same time and grow at the same rate, the size distribution of resulting particles will be in the narrow range. In these cases, the formation of smaller number of nuclei in the lower concentration, such as the product obtained with 0.12 g hydrazine hydrate, on account of the low nucleation rate would induce growth of particles and broad size distribution. At a very high concentration, such as in the presence of 0.36 g hydrazine hydrate, too many nuclei were formed at the same time and the solvation and the particle's surface potential cannot inhibit agglomeration [26]. This suggests that for the formation of Ni/CNFs, initial concentration of hydrazine hydrate can determine the particle size of the resulting product.

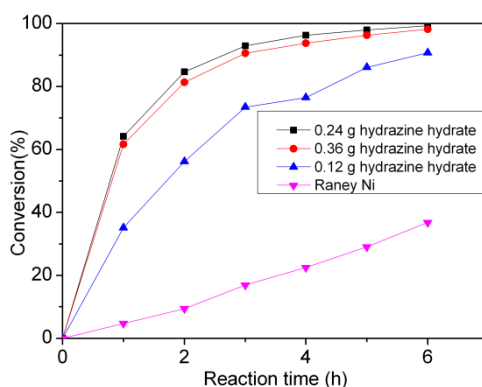


Fig.5. Catalytic activities of the Ni/CNFs prepared using various amounts of hydrazine hydrates.

Table 1 Hydrogenation activity of PNP over the Ni/CNFs prepared using various amounts of hydrazine hydrates at 2 h

Catalyst	Amount of hydrazine hydrate/g	Average particle size/nm	Conversion of PNP (%)	Selectivity for PAP (%)
Ni/CNFs	0.24	18.4	85	99
	0.36	27.3	83	99
	0.12	145	56	99

The catalytic activities of the Ni/CNFs are illustrated in Fig. 5. It can be seen that the selectivity of PNP to PAP was near 100% while the hydrogenation of PNP was catalyzed by all the

Ni/CNFs. At first 2 h, the PNP conversions were 85%, 83%, and 56% (Table 1) while the Ni/CNFs were prepared by using various amounts of hydrazine hydrates. After reaction for 6 h, the conversions of PNP were up to 99%, 98%, and 91%, respectively. By comparing the initial PNP hydrogenation rates at the first 2 h, it was found that the catalytic activities of the Ni/CNFs were increased with lessening of average particles size of nickel nanoparticle on the surface of CNFs. The reason for the sensitivity of catalytic activity to particle size is probably relative to the various point defects and surface area. The lesser particle sizes have higher surface area and more point defects caused by the fast nucleation, which is which may be responsible for the higher catalytic activity. To compare the catalytic activities of the as-prepared Ni/CNFs with that of RANEYs Ni catalyst, the catalytic activity of RANEYs Ni catalyst was also investigated. RANEYs Ni catalyst exhibited little catalytic activities under the same conditions. After reaction for 6 h, the conversion of PNP was only 37% (Fig. 5). Moreover, there was a byproduct produced and the selectivity of p-aminophenol was less than 95% while PNP hydrogenation was catalyzed by RANEYs Ni catalyst. The byproduct was ascribed to the product of benzene ring hydrogenation, which was caused by the micropores of RANEYs Ni. Obviously, all the Ni/CNFs showed higher catalytic activity and selectivity than the Raney Ni in the hydrogenation of PNP to PAP.

4. Conclusions

In this work, Ni/CNFs catalysts were prepared by a microwave-assisted procedure in a water/EG system. A dense and homogeneous layer of nickel nanoparticles with controllable size determined by initial concentration of hydrazine hydrate on the surface of CNFs can be obtained. The catalytic performance of Ni/CNFs in the hydrogenation of PNP revealed that all the prepared Ni/CNFs showed higher catalytic activity and selectivity in the hydrogenation of PNP to PAP compared with that of conventional Raney Ni catalyst. In addition, the catalytic activities of the Ni/CNFs were increased with lessening of average particles size of nickel nanoparticle on the surface of CNFs, but little influence on the selectivity.

Acknowledgements

This work was supported by the National Natural Science Foundation of China (11564011, 51362010), the Natural Science Foundation of Hainan Province (514207, 514212), the Scientific Research Projects of Colleges and Universities of Hainan Province (HNKY2014-14), the Scientific Research Projects of Hainan University (kyqd1502), and the Open Foundation of Key Laboratory of Advanced Materials of Tropical Island Resources (Hainan University), Ministry of Education (AM2017-20).

References

- [1] Z. J. Wu, J. Chen, Q. Di, M. H. Zhang, *Catalysis Communications*, **18**, 55 (2012).
- [2] M.A. Bhosale, D.R. Chenna, J.P. Ahire, B.M. Bhanage, *RSC Advances*, **5**(65), 52817 (2015).
- [3] D.P. Kumar, *RSC Advances*, **4**(85), 45449 (2014).
- [4] T. Komatsu, T. Hirose, *Applied Catalysis A: General*, **276**(1), 95 (2004).
- [5] Y. Du, H. L. Chen, R. Z. Chen, N. P. Xu, *Applied Catalysis A: General*, **277**(1), 259 (2004).
- [6] M. J. Vaidya, S. M. Kulkarni, R. V. Chaudhari, *Organic Process Research & Development*, **7**(2), 202 (2003).
- [7] H. Liu, J. Deng, W. Li, *Catalysis Letters*, **137**(3), 261 (2010).
- [8] A. L. Wang, H. B. Yin, H. H. Lu, J. J. Xue, M. Ren, T. S. Jiang, *Catalysis Communications*, **10**(15), 2060 (2009).
- [9] A. L. Wang, H. B. Yin, H. H. Lu, J. J. Xue, M. Ren, T. S. Jiang, *Langmuir*

- 25**(21), 12736 (2009).
- [10] A. L. Wang, H. B. Yin, M. Ren, H. H. Lu, J. J. Xue, T. S. Jiang, *New Journal of Chemistry*, **34**(4), 708 (2010).
- [11] I. H. A. E Maksod, E. Z. Hegazy, S. H. Kenawy, T. S. Saleh, *Applied Surface Science* **6**(255), 3471 (2009).
- [12] R. Z. Chen, Y. Du, W. H. Xing, N. P. Xu, *Chinese Journal of Chemical Engineering* **15**(6), 884 (2007).
- [13] H. H. Lu, H. B. Yin, Y. M. Liu, T. S. Jiang, L. B. Yu, *Catalysis Communications* **10**(3), 313 (2008).
- [14] C. Wang, J. S. Qiu, C. H. Liang, L. Xing, X. M. Yang, *Catalysis Communications* **9**(8), 1749 (2008).
- [15] P. L. Liu, H. Xie, S. R. Tan, K. Y. You, N. L. Wang, H. A. Luo, *Reaction Kinetics and Catalysis Letters* **97**(1), 101 (2009).
- [16] E. Ochoa-Fernández, D. Chen, Z. X. Yu, B. Tøtdal, M. Rønning, A. Holmen, *Catalysis Today* **102**, 45 (2005).
- [17] J. H. Bitter, M. K. van der Lee, A. G. T. Slotboom, A. J. van Dillen, K. P. de Jong, *Catalysis Letters* **89**(1-2), 139 (2003).
- [18] M. K. van der Lee, A. J. van Dillen, J. H. Bitter, K. P. de Jong, *The Journal of the American Chemical Society* **127**(39), 13573 (2005).
- [19] G. Z. Wang, Z. Gao, G. P. Wan, S. W. Lin, P. Yang, Y. Qin, *Nano Research*, **7**(5), 704 (2014).
- [20] G. Z. Wang, G. Ran, G. P. Wan, P. Yang, Z. Gao, S. W. Lin, C. Fu, Y. Qin, *ACS Nano* **8**(5), 5330 (2014).
- [21] G. Z. Wang, Z. Gao, S. W. Tang, C. Q. Chen, F. F. Duan, S. C. Zhao, S. W. Lin, Y. H. Feng, L. Zhou, Y. Qin, *ACS Nano* **6**(12), 11009 (2012).
- [22] F. L. Jia, L. Z. Zhang, X. Y. Shang, Y. Yang, *Advanced Materials* **20**(5), 1050 (2008).
- [23] G. Z. Wang, X. E. Peng, L. Yu, G. P. Wan, S. W. Lin, Y. Qin, *Journal of Materials Chemistry A* **3**(6), 2734 (2015).
- [24] S. Iftimie, R. Mallet, J. Merigeon, L. Ion, M. Girtan, S. Antohe, *Digest Journal of Nanomaterials and Biostructures* **10**(1), 221 (2015).
- [25] G. P. Wan, G. Z. Wang, X. Q. Huang, H. N. Zhao, X. Y. Li, K. Wang, L. Yu, X. E. Peng, Y. Qin, *Dalton Transactions* **44**(43), 18804 (2015).
- [26] A. M. El-Nahrawy, M. M. Elokr, F. Metawe, B. A. A. Osman, *Journal of Ovonic Research*, **12**(5), 253 (2016).